AEM
Journals.ASM.org

MS2 Virus Inactivation by Atmospheric-Pressure Cold Plasma Using Different Gas Carriers and Power Levels

Yan Wu,[a*] Yongdong Liang,[b] Kai Wei,[a] Wei Li,[b,c] Maosheng Yao,[a] Jue Zhang,[b,c] Sergey A. Grinshpun[d]

State Key Joint Laboratory of Environmental Simulation and Pollution Control, College of Environmental Sciences and Engineering, Peking University, Beijing, China[a]; College of Engineering, Peking University, Beijing, China[b]; Academy for Advanced Interdisciplinary Studies, Peking University, Beijing, China[c]; Center for Health-Related Aerosol Studies, University of Cincinnati, Cincinnati, Ohio, USA[d]

In this study, airborne MS2 bacteriophages were exposed for subsecond time intervals to atmospheric-pressure cold plasma (APCP) produced using different power levels (20, 24, and 28 W) and gas carriers (ambient air, Ar-O_2 [2%, vol/vol], and He-O_2 [2%, vol/vol]). In addition, waterborne MS2 viruses were directly subjected to the APCP treatment for up to 3 min. MS2 viruses with and without the APCP exposure were examined by scanning electron microscopy (SEM), reverse transcription-PCR (RT-PCR), and sodium dodecyl sulfate-polyacrylamide gel electrophoresis (SDS-PAGE). Viral inactivation was shown to exhibit linear relationships with the APCP generation power and exposure time ($R^2 > 0.95$ for all energy levels tested) up to 95% inactivation (1.3-log reduction) after a subsecond airborne exposure at 28 W; about the same inactivation level was achieved for waterborne viruses with an exposure time of less than 1 min. A larger amount of reactive oxygen species (ROS), such as atomic oxygen, in APCP was detected for a higher generation power with Ar-O_2 and He-O_2 gas carriers. SEM images, SDS-PAGE, and agarose gel analysis of exposed waterborne viruses showed various levels of damage to both surface proteins and their related RNA genes after the APCP exposure, thus leading to the loss of their viability and infectivity.

Inhalation of microbial aerosol particles can cause various health effects, ranging from moderate respiratory impairments to death (1–3). Studies showed that large-scale infectious disease outbreaks, such as the outbreaks of severe acute respiratory syndrome in 2003 and influenza virus H1N1 in 2009, were triggered by airborne transmission of the viral agents (4–7). To reduce exposure to viruses, various methods have been developed and evaluated, including UV irradiation (8–11), chemical agents (12), electrical fields (13, 14), ion emission (15–18), ozone generation (19), and microwave irradiation (20–23). In recent years, atmospheric-pressure cold plasma (APCP), a low-temperature decontamination technology, has gained increased attention for the inactivation of microbial agents due to its high degree of effectiveness and low cost (24). APCP is known as the fourth state of matter, which consists of free charged ions and radicals moving in random directions. Although APCP has been extensively applied to the inactivation of liquid-borne or surface-borne agents (25–30), only a few inactivation studies exposing airborne microbial agents to APCP have been conducted (31–34). A recent study reported that a significant fraction (>85%) of airborne bacteria and fungi from both indoor and outdoor environments lost their viability within 60 ms of exposure to APCP (34). Reactive oxygen species (ROS) such as OH· were observed in the plasma produced using the air carrier, and bacterial membrane damage was detected in APCP-treated samples (34). Zimmermann et al. (2011) studied the inactivation of adenoviruses in a liquid suspension using APCP; up to a 6-decimal-log reduction was achieved following a 4-min exposure (35). In another study, a more than 7-decimal-log reduction of surface-borne MS2 viruses resulted from a 9-min exposure to the APCP produced using a helium-oxygen (0.75%, vol/vol) gas mixture (36). That study also reported a positive association between the percentage of oxygen in the mixture and the virus inactivation rate (36). To our best knowledge, the APCP technology has yet to be applied to the *in situ* inactivation of airborne viruses.

This study was designed to investigate the effects of APCP on both airborne and waterborne MS2 viruses under different experimental conditions and, further, to elucidate the mechanisms by studying possible damage to RNA genes, the viral surface, and also surface proteins using reverse transcription (RT)-PCR and gel electrophoresis, as well as sodium dodecyl sulfate-polyacrylamide gel electrophoresis (SDS-PAGE). The results provide guidance on the use of APCP as an alternative for combating viral threats.

MATERIALS AND METHODS

Preparation of MS2 suspensions. The aerosolized MS2 bacteriophage (ATCC 15597-B1) served as the challenge viral aerosol in this study. The double-top-agar-layer plaque technique described previously (37) was utilized to propagate MS2 virus using *Escherichia coli* (ATCC 15597) as the host organism. After culturing and washing, the sterile water containing the MS2 phages was decanted into a sterile 25-ml tube (Corning, Inc., Corning, NY, USA) and further centrifuged at 5,000 × *g* for 30 min to

Received 11 October 2014 **Accepted** 17 November 2014

Accepted manuscript posted online 21 November 2014

Citation Wu Y, Liang Y, Wei K, Li W, Yao M, Zhang J, Grinshpun SA. 2015. MS2 virus inactivation by atmospheric-pressure cold plasma using different gas carriers and power levels. Appl Environ Microbiol 81:996–1002. doi:10.1128/AEM.03322-14.

Editor: J. Björkroth

Address correspondence to Maosheng Yao, yao@pku.edu.cn, or Jue Zhang, zhangjue@pku.edu.cn.

Y.W.,Y.L., and K.W. contributed equally to this article.

* Present address: Yan Wu, SINBERBEST Program, Berkeley Education Alliance for Research in Singapore (BEARS), and School of Civil and Environmental Engineering, Nanyang Technological University, Singapore.

Supplemental material for this article may be found at http://dx.doi.org/10.1128/AEM.03322-14.

doi:10.1128/AEM.03322-14

The authors have paid a fee to allow immediate free access to this article.

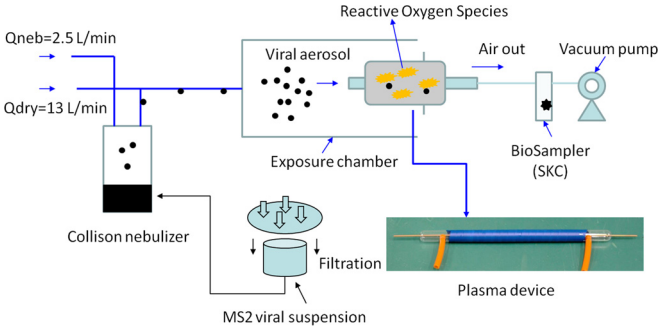

FIG 1 Experimental setup for investigation of aerosolized MS2 viruses exposed to APCP produced using different gas carriers (ambient air, Ar-O_2 [2%, vol/vol], and He-O_2 [2%, vol/vol]) and power levels (20, 24, and 28 W); a photo of the plasma generator used for inactivation of airborne viruses is shown at the bottom right.

remove *E. coli* and the agar debris. The resulting phage pellet was resuspended in sterile water and stored at 4°C. Fresh phage suspensions were prepared for each experiment, in which both exposure and control (without plasma treatment) runs used the same batch of MS2.

Experimental procedures. (i) Exposure of airborne MS2 to APCP. The experimental setup used in this study is schematically presented in Fig. 1. The main elements include a Collison nebulizer (BGI Inc., Waltham, MA, USA), used for aerosolizing viruses from the MS2 suspension; an APCP generation device; and a BioSampler apparatus (SKC, Inc., Eighty Four, PA, USA), operating at 12.5 liters/min, for collecting viruses from the air. Here, we tested the APCP generator described in a previous work (34) and shown in Fig. 1 at three generation power levels: 20, 24, and 28 W. In our study, the chosen plasma generation power levels of 20, 24, and 28 W correspond, respectively, to the following three voltage and current sets: 30 V and 0.68 A, 30 V and 0.8 A, and 30 V and 0.93 A. The wave forms of the applied currents and voltages are presented in Fig. S1 to S3 in the supplemental material.

During the exposure, the MS2 viruses were continuously aerosolized at a nebulizer flow rate (Q_{neb}) of 2.5 liters/min using nitrogen gas (N_2), and the viral aerosols were delivered to the exposure test chamber by an additional dry N_2 flow rate (Q_{dry}) of 13 liters/min. Inside the chamber, the viral aerosol was exposed to the APCP generated using three different generation power levels and three different gas carriers, including ambient air, He-O_2 (2%, vol/vol), and Ar-O_2 (2%, vol/vol). On the basis of the dimensions of the plasma generation device and the exit flow rate (equal to the BioSampler's sampling flow rate of 12.5 liters/min), the exposure time for the virions inside the plasma device was calculated to be 0.12 s. Each of the exposed and control viral aerosol samples was continuously collected for 20 min. The BioSampler was charged with 20 ml of deionized (DI) water (Millipore Corporation, Billerica, MA, USA). The sampling flow rate was calibrated using a mini-Buck calibrator (A. P. Buck, Inc., Orlando, FL, USA) prior to each test.

The viral aerosol samples collected with and without the APCP treatment were cultured for 1 to 2 days at 37°C using the double-top-agar-layer technique. The viruses were enumerated by manual counting of the number of PFU. Using the flow rate and the processing time, the culturable viral aerosol concentration (number of PFU/m^3) was determined. For each set of conditions, the viral aerosol inactivation experiment was conducted in three replicates. After sample collection, plasma discharge was performed between consecutive replicate tests alternated every 30 min. Viral aerosol particle charging was not used during the treatment.

The rate of viral survival, *S*, was calculated using the following equation:

$$S = (\mathrm{PFU}_{\mathrm{exposed}}/\mathrm{PFU}_{\mathrm{control}}) \times 100 \quad (1)$$

where $\mathrm{PFU}_{\mathrm{exposed}}$ and $\mathrm{PFU}_{\mathrm{control}}$ are the culturable viral aerosol concentrations (in number of PFU) with and without the APCP treatment, respectively.

(ii) Exposure of waterborne MS2 viruses to APCP. In this part of the study, the same MS2 bacteriophage was treated with APCP while in suspension (not airborne); additionally, the testing examined longer exposure time intervals up to 3 min. The originally prepared MS2 bacteriophage was serially diluted; dilution factors were 10^{-1} and 10^{-2}. In these experiments, 200 μl of viral suspensions with different concentrations was added into the wells of a 96-well plate with 3 replicates. Subsequently, the suspensions were exposed to the APCP produced using a microjet plasma generation device (38) at power levels of 20, 24, and 28 W and exposure times of 30, 60, 120, and 180 s. In the microjet plasma generator, two metal electrodes were separated from each other by a dielectric layer with a thickness of 0.5 mm. The openings in the two electrodes were 0.8 mm in diameter. One electrode was completely embedded in the device and powered by a direct current (DC) power supply (Matsusada Precision Inc., Shiga, Japan), and the other electrode was grounded for safety. Only negative high voltage was tested for this study. As described previously, the discharge sustaining voltage ranged from approximately 400 to 800 V with an operating current in the range of 20 to 35 mA (38). The flow rate of the gas carrier used for the liquid samples was 5 liters/min. Under these operating conditions, a plasma jet of 15 mm was generated in the liquid. Figure S4 in the supplemental material shows the temperature profile, measured using thermal imaging infrared cameras (FLIR Systems, Inc.), for the liquid suspension treated by the microjet plasma generation device in inactivating liquid-borne MS2 viruses. As observed from Fig. S4, the temperature in the liquid suspension ranged from 26.7°C to 36.2°C.

For each set of experimental conditions, the exposure control test was conducted in three replicates, and the viral survival rates were determined using equation 1, provided above, and used for airborne inactivation experiments. In addition, the damage to MS2 viral RNA genes was investigated using waterborne MS2 viruses with the APCP treatment. Agarose gel electrophoresis combined with RT-PCR was applied for analyzing the effects of the plasma treatment on these RNA genes. The extraction of viral RNA was performed following the procedure described in our previous study (37). The cDNA, the forward primers, and the reverse primers used in the previous work (37) were utilized here for amplifying viral surface protein genes: the A (maturation) protein gene (934 bp), capsid (coat) protein gene (160 bp), replicase protein gene (937 bp), and lysis protein gene (114 bp) (39, 40). The RT-PCR cycle conditions were set to the following: 50°C for 30 min (reverse transcription); 94°C for 2 min; 40 cycles in which each cycle included denaturation at 94°C for 1 min, annealing at 55°C for 1 min, and extension at 65°C for 2 min; and, finally, an extension at 65°C for 10 min (37). DI water served as the negative control in the RT-PCR experiments. Agarose gel electrophoresis was performed with the RT-PCR products and Sub-Cell GT instruments (Bio-Rad, Hercules, CA, USA) according to the manufacturer's instructions. For the gel analysis, approximately 20 μl RT-PCR product was added to each designated well of 3% agarose gels. Gel electrophoresis was performed at a constant voltage of 60 V for 100 min, and then the gels were stained using GelRed solution (diluted 10^4 times with DI water; Biotium, Hayward, CA, USA) and photographed using a Molecular Imager Gel Doc XR system (Bio-Rad, Hercules, CA, USA) at a wavelength of 254 nm under a UV lamp. In this effort, we did not use a real-time RT-quantitative PCR; thus, the results obtained here represent only those of a semiquantitative analysis of the damaged RNA genes for viruses inactivated by APCP.

To further investigate the mechanism of viral inactivation by APCP, we employed SDS-PAGE. The gel was prepared using a kit following the manufacturer's instruction (Realtimes Beijing Biotechnology Co., Ltd., Beijing, China). For the electrophoresis buffer, 1× Tris-glycine in a total volume of 300 ml was used. The MS2 viruses were treated with APCP for 3 min at a generation power level of 28 W. A volume of 10 μl of suspension containing either control or treated MS2 virus and a protein ladder (10 to 170 kDa) was separately added to the prepared gel and subjected to SDS-PAGE analysis using vertical electrophoresis equipment (model number

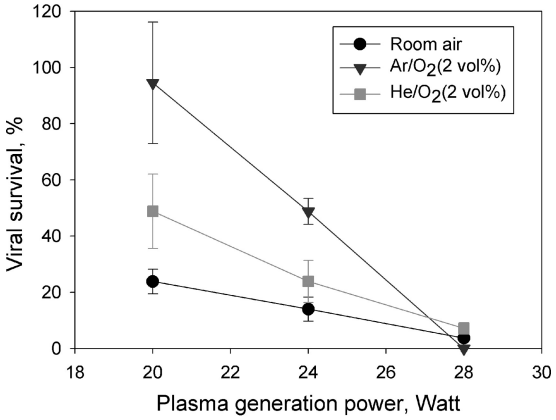

FIG 2 Survival of airborne MS2 viruses exposed to the APCP produced at different power levels with different gas carriers. The estimated exposure time was 0.12 s. Data points and error bars represent, respectively, the averages and standard deviations from three independent measurements.

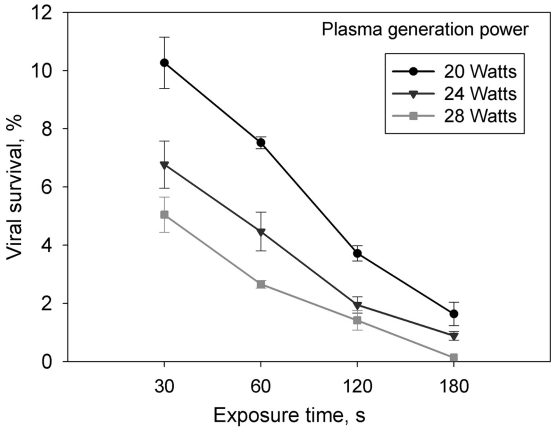

FIG 3 Survival of waterborne MS2 viruses as a function of the APCP exposure time at different power levels with ambient air as the plasma gas carrier. Data points and error bars represent, respectively, the average values and standard deviations from three independent measurements.

DYY-12; Beijing Liuyi Instrument Factory, Beijing, China) operated at a voltage of 80 V for 15 min and then at a voltage of 120 V for 90 min. After the experiments, the gel was stained using the silver stain agent (Beijing ComWin Biotech Co., Ltd., Beijing, China).

Statistical analysis. The experimental data, including rates of survival under different gas carriers, plasma generation power levels, and exposure times, were statistically analyzed using one-way analysis of variance (ANOVA), an independent *t* test, and linear regression analysis. *P* values below 0.05 indicated a statistically significant difference.

RESULTS

Airborne inactivation. Overall, the APCP exposure significantly decreased the levels MS2 virus survival for both the airborne and liquid-borne states. Figure 2 shows the survival of the aerosolized viruses when exposed to the APCP produced using different power levels and gas carriers. Regardless of the gas carrier type, the survival of MS2 viruses was observed to decrease with increasing power levels (for all comparisons, $P < 0.05$ by ANOVA). On the other hand, for a given plasma generation power level, the loss of viability of aerosolized viruses strongly depended on the gas carrier type (for all comparisons, $P < 0.0001$ by ANOVA). The data from Fig. 2 suggest that the ambient air carrier produced the highest level of inactivation at power levels of 20 and 24 W, followed by the gas carriers Ar-O_2 (2%, vol/vol) and He-O_2 (2%, vol/vol). In contrast, at a power level of 28 W, the Ar-O_2 (2%, vol/vol) mixture was found to be the most efficient in inactivating aerosolized viruses, followed by ambient air and He-O_2 (2%, vol/vol). The APCP treatment performed using ambient air as the gas carrier at 28 W for 0.12 s inactivated more than 95% (1.3-log reduction) of the viruses in the air. At the same power level, APCP with Ar-O_2 (2%, vol/vol) was not as efficient, inactivating only <50% (0.3-log reduction) of viruses. At 20 W, the inactivation produced by Ar-O_2 (2%, vol/vol) was as low as <10% (0.05-log reduction); however, surprisingly, it increased to approximately 100% (negligibly low survival) when the power level increased from 20 to 28 W (Fig. 2). With Ar-O_2 (2%, vol/vol), the viral viability loss was even higher than the one achieved with ambient air at the same power level. From the linear regression analysis, we concluded that APCP with Ar-O_2 (2%, vol/vol) features the highest dependency of its viral aerosol inactivation on the power level, followed by plasma with He-O_2 (2%, vol/vol) and ambient air as gas carriers.

Waterborne inactivation. Constrained by the size of the plasma generation device available and the exit flow rate of 12.5 liters/min, the aerosol exposure time tested here was rather short (about 0.12 s). To extend the plasma exposure time, waterborne MS2 viruses were used for further tests. As seen in Fig. 3, the survival of waterborne MS2 viruses decreased as the exposure time increased from 30 to 180 s, when APCP was produced using the ambient air carrier at different power levels. Similar to the results of the experiments with aerosolized viruses, an increase in the power level was shown to decrease the survival of waterborne MS2 viruses (Fig. 3). Linear regression analysis indicated that there was a strong association between the exposure time and survival; i.e., a longer exposure time corresponded to lower survival of the waterborne MS2 viruses ($R^2 > 0.95$ for all energy levels). Similar results were observed with other gas carriers, such as Ar-O_2 (2%, vol/vol) and He-O_2 (2%, vol/vol), as shown in Fig. S5 and S6 in the supplemental material. The differences in survival and dependence on power level for different gas carriers can be attributed to the different rates of ROS generation arising from the different atomic structures of the carriers. Overall, APCP treatment of a viral suspension for >30 s resulted in a rate of survival of <20% (>0.69-log reduction) for all tested gas carriers and power levels (Fig. 3; see also Fig. S5 and S6 in the supplemental material). The differences in inactivation resulting from different gas carrier types were likely due to the interaction of MS2 viruses with different plasma chemistries; additionally, the discrepancy may be associated with the different die-off times of the ROS and the charged particles released from the APCP.

Inactivation mechanisms. Figure 4 presents the data obtained by analyzing the APCP chemistry produced under different gas carriers and power levels. Optical emission spectroscopy (OES) identified the ROS, such as O (atomic oxygen), in the emission peaks when testing was done with gas carriers such as Ar-O_2 (2%, vol/vol) and He-O_2 (2%, vol/vol). From the data presented in Fig. 4, it can be seen that the amount of O increased with increasing plasma generation power level. Typically, the plasma produced using Ar-O_2 (2%, vol/vol) had higher emission peaks of ROS in the emission spectra than the one generated with He-O_2 (2%, vol/vol). This, in turn, resulted in rates of virus survival with

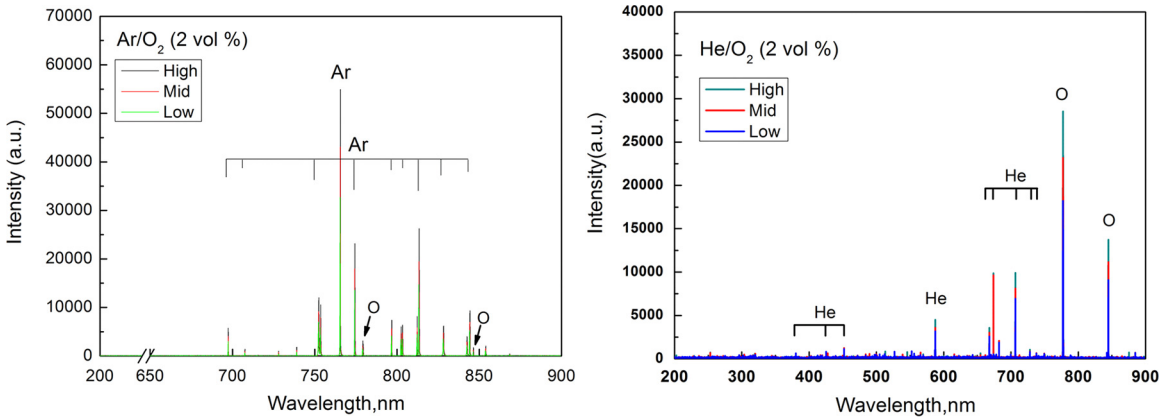

FIG 4 Optical emission spectroscopy (OES) image of the APCP generated with the plasma device shown in Fig. 1. Gas carriers are Ar-O_2 (2%, vol/vol) and He-O_2 (2%, vol/vol); plasma generation power levels were low (20 W), medium (a middle level [Mid]; 24 W), and high (28 W). a.u., arbitrary units.

He-O_2 (2%, vol/vol) higher than those found with Ar-O_2 (2%, vol/vol) (see Fig. S1 and S2 in the supplemental material). Among the ROS, the hydroxyl radicals (·HO) represent the most reactive form; accordingly, a lower rate of viral survival was observed with the APCP produced using ambient air than the APCP produced using the two other gas carriers. This result is consistent with those for the airborne and waterborne virus exposures seen in Fig. 2 and 3, respectively.

To further develop a mechanistic understanding of the inactivation of MS2 viruses due to exposure to the APCP, we examined the control (untreated) and plasma-treated viral suspension samples using a scanning electron microscope. The MS2 virion size is about 27 nm (39), while MS2 RNA is tightly compacted within the virion and confined to a radius of 8.3 ± 1 nm (40). In contrast, the MS2 coat protein shell is approximately 13.6 ± 2 nm in size and has a thickness of 2.1 ± 1 nm (40). As seen from Fig. 5, the images of virions exposed to the plasma treatment show more fragments than nonexposed samples, which show spherical particles. Nonetheless, due to the low resolution, the detailed surface damage might not be immediately identified from the images. In contrast, damage to the viral RNA genes that code for four major viral surface proteins, the maturation protein (A protein), the capsid protein, the replicase protein, and the lysis protein, was confirmed (Fig. 6). Figure 6 shows the results of agarose gel electrophoresis of viral RNA genes coding for surface proteins of waterborne MS2 viruses upon plasma exposure over 30, 60, 120, and 180 s at a power level of 24 W when ambient air served as the gas carrier. The RT-PCR products were detected in the target bands, and the gel band intensity data generally suggest a positive association between the time of exposure to APCP and the degree of gene damage. One exception was the reappearance of the replicase protein gene with 120 s exposure, which was unexpected and might have

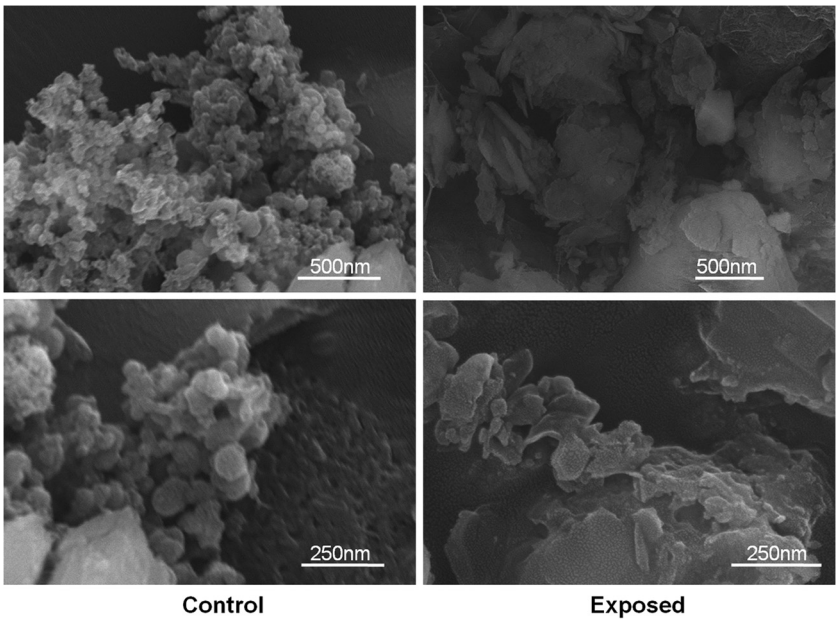

FIG 5 Scanning electron microscope images of waterborne MS2 viruses treated and untreated with the APCP. The gas carrier was ambient air, the plasma generation power was 24 W, and the exposure time was 120 s.

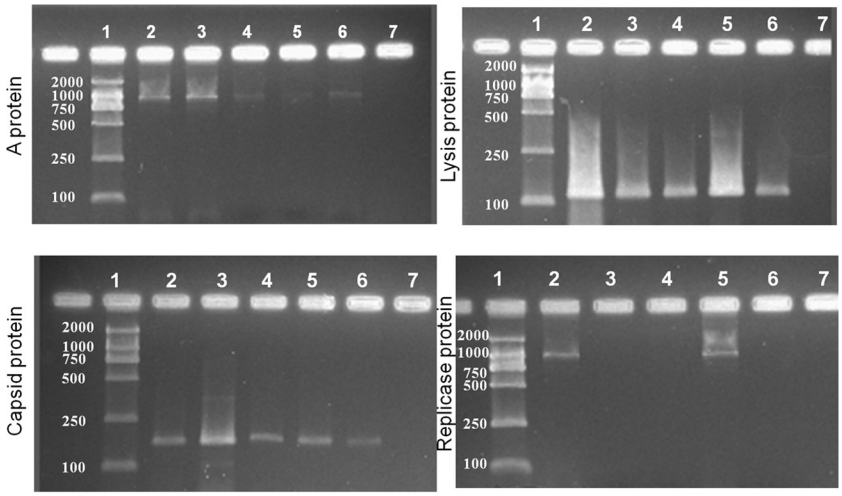

FIG 6 Image of gel after agarose gel electrophoresis of viral RNA genes coding for the surface proteins A protein, capsid protein, replicase protein, and lysis protein of waterborne MS2 viruses. The gas carrier was ambient air, the plasma generation power was 24 W, and the time of exposure to plasma was 30, 60, 120, or 180 s. Lanes: 1, D2000 marker (numbers on the left are molecular sizes [in base pairs]; 2, MS2-positive control; 3, time of exposure of 30 s; 4, time of exposure of 60 s; 5, time of exposure of 120 s; 6, time of exposure of 180 s; 7, negative control (DI water).

been caused by the nonuniform plasma exposure to the viral suspension due to the airflow used to produce the plasma. In general, damage to the maturation and replicase genes made the virus unable to express the related proteins, which impeded its ability to seek the host and replicate. For example, even if all the surface proteins are intact after the APCP treatment, damage solely to the RNA genes may prevent the virus from replicating inside the host. In addition to damage to RNA genes, the plasma exposure could also have caused damage to surface proteins.

For MS2 viruses, the following proteins are known to exist on its surface: the maturation protein (40 kDa), the coat protein (13.86 kDa), the replicase protein (60 kDa), and the lysis protein (8.87 kDa) (39, 40). To study the effects of APCP on these surface proteins, SDS-PAGE of the APCP-treated MS2 viruses was conducted. Replicase protein (red arrow) and maturation protein (blue arrow) were observed on the SDS-polyacrylamide gel image (Fig. 7). Overall, we have found from the SDS-polyacrylamide gel image (Fig. 7) that with exposure to APCP the band intensity for both the replicase and maturation proteins decreased; e.g., it was barely seen for the maturation protein after the 180-s exposure. Also observed from Fig. 7, some bands disappeared after the APCP exposure. These data suggest that the APCP exposure can significantly degrade the MS2 viral surface proteins. Because the capsid and lysis proteins have smaller sizes, they were not clearly separated by SDS-PAGE under the conditions applied in this work.

DISCUSSION

The differences in viral survival levels observed in this study for different gas carriers can be linked mainly to the differences in plasma chemistry. It has recently been reported that an increase of the oxygen concentration in the mixture of H_2 and O_2 from 0.25% to 0.75% generated a >1.5-fold increase in the level of inactivation of surface-borne MS2 viruses (36). A >99% (>2-log reduction) inactivation of waterborne MS2 viruses was achieved in this study as a result of their 3-min exposure to ACPC with He-O_2 (2%, vol/vol) (see Fig. S6 in the supplemental material), and such an efficiency may be further enhanced by optimizing the oxygen concentration. For example, a selected oxygen percentage of between 0.5% and 1.5% in the He-O_2 gas carrier was reported to produce high levels of atomic oxygen (41). Ambient air with an oxygen content of approximately 21% has a composition vastly different from that of the two other carriers utilized in this study. Accordingly, different reactive products are released. In a previous work (34), hydroxyl radicals rather than atomic oxygen were observed earlier when generating APCP with the ambient air carrier. As shown in Fig. S4 in the supplemental material, the highest temperature generated in the liquid suspension was about 36.2°C, and such a temperature does not affect the viability of the viruses.

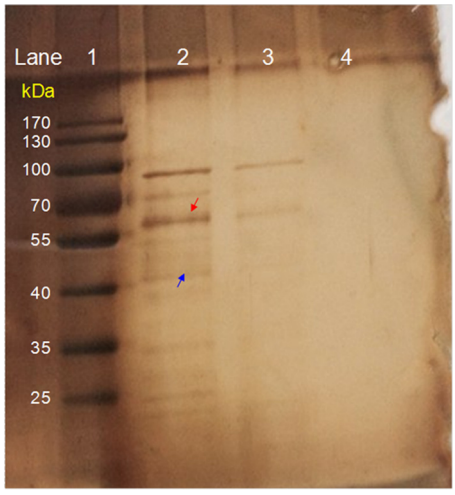

FIG 7 SDS-polyacrylamide gel image of the APCP-treated and untreated (control) MS2 viral surface proteins. The plasma was generated with the device used to test waterborne viruses, the plasma generation power was 28 W, and the time of exposure was 180 s. Lanes: 1, protein ladder; 2, untreated MS2 virus control; 3, plasma-treated MS2 viral proteins; 4, negative control (DI water). Red arrow, replicase protein (60 kDa); blue arrow, maturation protein (40 kDa).

Therefore, the inactivation of MS2 viruses by APCP that we documented here was primarily associated with the generated ROS, such as hydroxyl radicals and atomic oxygen, and not the heat generated from the plasma device. These species could have reacted with RNA genes, resulting in their damage (Fig. 6). The ROS generated from the plasma is described to be able to break structurally important bonds of peptidoglycan (i.e., C—O, C—N, or C—C bonds) and to lead to the destruction of the bacterial cell wall (42). Alternative causes may also be present. For example, one study pointed out that the plasma inactivation of lambda phage occurred mainly due to the damage to the coat protein, while its DNA damage at early stages was negligible (43).

Here, we observed damage to the surface proteins; i.e., the band intensity was significantly decreased compared to that for the control or disappeared, as seen in Fig. 7. A previous study has shown that the A protein is exposed to the capsid surface and directly binds the MS2 genomic RNA at its 5′ and 3′ ends (40). In addition to RNA packing, the main function of the A protein of an MS2 virion is to identify the host. In contrast, the viral replicase and lysis proteins are involved in the replication and lysis of *E. coli* bacteria, respectively (40). Therefore, any damage to the A (maturation) and replicase proteins from the external assault would result in the loss of virus infectivity as well as RNA packing. On the other hand, the MS2 coat protein, the primary structural protein shell, has a total of 90 homodimers arranged in a quasiequivalent T=3 lattice on the capsid surface (44). The MS2 coat protein was shown to bind a stem-loop structure in viral RNA for both encapsidation of the genome and translational repression of replicase synthesis (44). Besides, the coat protein is reported to interact with MS2 RNA at 20 sites along the RNA backbone (44). Unfortunately, in this study, the bands for lysis and coat proteins did not show up in the gel due to their small sizes. Nonetheless, damage to the coat proteins would affect the infection ability of the MS2 viruses.

In this study, we have observed a significant inactivation of MS2 viruses resulting from their exposure to APCP. The data suggest that the inactivation of the MS2 viruses for both the airborne and waterborne states depends on the power level, exposure time, and gas carrier. The viral inactivation process is primarily attributed to the ROS released from APCP, including damage to the virus surface proteins and RNA genes. Although the magnitude of the effect of APCP ROS is generally higher than that present in the atmosphere, results presented here can facilitate a better understanding of virus decay in ambient air. Future research efforts should be directed toward determining the efficiency of APCP against human viral pathogens, such as H1N1 and H7N9 influenza viruses and even Ebola virus. Owing to its complex contents, e.g., an assembly of photons, electrons, positive and negative ions, free radicals, and excited or nonexcited molecules and atoms (34, 45), the currently achieved understanding of the biological mechanism of APCP-induced viral inactivation is rather limited, and this work contributes to the development of a better understanding of viral inactivation when viruses are in contact with APCP. Clearly, the APCP technology has advantages over chemical methods with respect to secondary environmental pollution and cost (12), and the information obtained here will also serve as a foundation for developing efficient plasma-based technologies and strategies to control viral agents.

ACKNOWLEDGMENTS

This study was supported by the NSF of China (grants 41121004, 21277007, and 21477003), the Ministry of Science and Technology (grant 2015CB5534), and the Ministry of Education (grant 20130001110044).

S.A.G. was extensively involved in discussion and interpretation of the data and the writing of the manuscript.

REFERENCES

1. **World Health Organization.** 2014. Influenza (seasonal) 2014. World Health Organization, Geneva, Switzerland. http://www.who.int/mediacentre/factsheets/fs211/en/index.html. Accessed 9 May 2014.
2. **Robbins CA, Swenson LJ, Nealley ML, Gots RE, Kelman BJ.** 2000. Health effects of mycotoxins in indoor air: a critical review. Appl Occup Environ Hyg **15:**773–784. http://dx.doi.org/10.1080/10473220050129419.
3. **Douwes J, Thorne P, Pearce N, Heederik D.** 2003. Bioaerosol health effects and exposure assessment: progress and prospects. Ann Occup Hyg **3:**187–200. http://dx.doi.org/10.1093/annhyg/meg032.
4. **Yu ITS, Li Y, Wong TW, Tam W, Chan ATY, Lee JHW, Leung YC, Ho T.** 2004. Evidence of airborne transmission of the severe acute respiratory syndrome virus. N Engl J Med **351:**1731–1739. http://dx.doi.org/10.1056/NEJMoa040694.
5. **Majić Z, Jukić I, Pavlin S.** 2009. Air transport and logistics in pandemic outbreak of influenza A (H1N1) virus. PROMET Traffic Transport **21:**441–450. http://dx.doi.org/10.7307/ptt.v21i6.258.
6. **Baker MG, Thornley CN, Mills C, Roberts S, Perera S, Peters J, Kelso A, Barr I, Wilson N.** 2010. Transmission of pandemic A/H1N1 2009 influenza on passenger aircraft: retrospective cohort study. BMJ **340:**c2424. http://dx.doi.org/10.1136/bmj.c2424.
7. **Tellier R.** 2009. Aerosol transmission of influenza A virus: a review of new studies. J R Soc Interface **6**(Suppl 6):S783–S790. http://dx.doi.org/10.1098/rsif.2009.0302.focus.
8. **Ryan K, McCabe K, Clements N, Hernandez M, Miller SL.** 2010. Inactivation of airborne microorganisms using novel ultraviolet radiation sources in reflective flow-through control devices. Aerosol Sci Technol **44:**541–550. http://dx.doi.org/10.1080/02786821003762411.
9. **Peccia J, Werth HM, Miller S, Hernandez M.** 2001. Effects of relative humidity on the ultraviolet induced inactivation of airborne bacteria. Aerosol Sci Technol **35:**728–740. http://dx.doi.org/10.1080/02786820152546770.
10. **Thurston-Enriquez JA, Haas CN, Jacangelo J, Riley K, Gerba CP.** 2003. Inactivation of feline calicivirus and adenovirus type 40 by UV radiation. Appl Environ Microbiol **69:**577–582. http://dx.doi.org/10.1128/AEM.69.1.577-582.2003.
11. **Gerba CP, Gramos DM, Nwachuku N.** 2002. Comparative inactivation of enteroviruses and adenovirus 2 by UV light. Appl Environ Microbiol **68:**5167–5169. http://dx.doi.org/10.1128/AEM.68.10.5167-5169.2002.
12. **Pottage T, Macken S, Giri K, Walker JT, Bennett AM.** 2012. Low-temperature decontamination with hydrogen peroxide or chlorine dioxide for space applications. Appl Environ Microbiol **78:**4169–4174. http://dx.doi.org/10.1128/AEM.07948-11.
13. **Kettleson EM, Ramaswami B, Hogan CJ, Jr, Lee MH, Biswas P, Angenent LT.** 2009. Airborne virus capture and inactivation by an electrostatic particle collector. Environ Sci Technol. **43:**5940–5946. http://dx.doi.org/10.1021/es803289w.
14. **Yao M, Mainelis G, An HR.** 2005. Inactivation of microorganisms using electrostatic fields. Environ Sci Technol **39:**3338–3344. http://dx.doi.org/10.1021/es048808x.
15. **Lee BU, Yermakov M, Grinshpun SA.** 2004. Removal of fine and ultrafine particles from indoor air environments by the unipolar ion emission. Atmos Environ **38:**4815–4823. http://dx.doi.org/10.1016/j.atmosenv.2004.06.010.
16. **Grinshpun SA, Adhikari A, Lee BU, Trunov M, Mainelis G, Yermakov M, Reponen T.** 2004. Indoor air pollution control through ionization, p 689–704. *In* Brebbia CA (ed), Air pollution: modeling, monitoring and management of air pollution. WIT Press, Southampton, United Kingdom.
17. **Agranovski IE, Huang R, Pyankov OV, Altman IS, Grinshpun SA.** 2006. Enhancement of the performance of low-efficiency HVAC filters due to continuous unipolar ion emission. Aerosol Sci Technol **40:**963–968. http://dx.doi.org/10.1080/02786820600833203.
18. **Huang R, Agranovski IE, Pyankov OV, Grinshpun SA.** 2008. Removal of viable bioaerosol particles with a low-efficiency HVAC filter enhanced by

continuous emission of unipolar air ions. Indoor Air **18:**106–112. http://dx.doi.org/10.1111/j.1600-0668.2007.00512.x.
19. **Tseng CC, Li CS.** 2006. Ozone for inactivation of aerosolized bacteriophages. Aerosol Sci Technol **40:**683–689. http://dx.doi.org/10.1080/02786820600796590.
20. **Wu Y, Yao M.** 2010. Inactivation of bacteria and fungus aerosols using microwave irradiation. J Aerosol Sci **41:**682–693. http://dx.doi.org/10.1016/j.jaerosci.2010.04.004.
21. **Wu Y, Yao M.** 2011. Effects of microwave irradiation on concentration, diversity and gene mutation of culturable airborne microorganisms of inhalable sizes in different environments. J Aerosol Sci **42:**800–810. http://dx.doi.org/10.1016/j.jaerosci.2011.07.002.
22. **Woo MH, Grippin A, Wu CY, Wander J.** 2012. Microwave-irradiation-assisted HVAC filtration for inactivation of viral aerosols. Aerosol Air Qual Res **12:**295–303. http://dx.doi.org/10.4209/aaqr.2011.11.0193.
23. **Zhang Q, Damit B, Welch J, Park H, Wu CY, Sigmund W.** 2010. Microwave assisted nanofibrous air filtration for disinfection of bioaerosols. J Aerosol Sci **41:**880–888. http://dx.doi.org/10.1016/j.jaerosci.2010.06.001.
24. **Kong MG, Kroesen G, Morfill G, Nosenko T, Shimizu T, Van Dijk J, Zimmermann JL.** 2009. Plasma medicine: an introductory review. New J Phys **11:**115012. http://dx.doi.org/10.1088/1367-2630/11/11/115012.
25. **Laroussi M, Mendis DA, Rosenberg M.** 2003. Plasma interaction with microbes. New J Phys **5:**1–10. http://dx.doi.org/10.1088/1367-2630/5/1/301.
26. **Chen CW, Lee HM, Chen SH, Chen HL, Chang MB.** 2009. Ultrasound-assisted plasma: a novel technique for inactivation of aquatic microorganisms. Environ Sci Technol **43:**4493–4497. http://dx.doi.org/10.1021/es900345z.
27. **Dobrynin D, Fridman G, Mukhin Y, Wynosky-Dolfi M, Rieger J, Rest R, Gutsol AF, Fridman A.** 2010. Cold plasma inactivation of *Bacillus cereus* and *Bacillus anthracis* (anthrax) spores. IEEE Trans Plasma Sci **38:**1878–1884. http://dx.doi.org/10.1109/TPS.2010.2041938.
28. **Fridman G, Brooks AD, Balasubramanian M, Fridman A, Gutsol A, Vasilets VN, Ayan H, Friedman G.** 2007. Comparison of direct and indirect effects of non-thermal atmospheric-pressure plasma on bacteria. Plasma Processes Polym **4:**370–375. http://dx.doi.org/10.1002/ppap.200600217.
29. **Ermolaeva SA, Varfolomeev AF, Chernukha MY, Yurov DS, Vasiliev MM, Kaminskaya AA, Moisenovich MM, Romanova JM, Murashev AN, Selezneva II, Shimizu T, Sysolyatina EV, Shaginyan IA, Petrov OF, Mayevsky EI, Fortov VE, Morfill GE, Naroditsky BS, Gintsburg AL.** 2011. Bactericidal effects of non-thermal argon plasma in vitro, in biofilms and in the animal model of infected wounds. J Med Microbiol **60:**75–83. http://dx.doi.org/10.1099/jmm.0.020263-0.
30. **Moreaua M, Orangea N, Feuilloley MGJ.** 2008. Non-thermal plasma technologies: new tools for bio-decontamination. Biotechnol Adv **26:**610–617. http://dx.doi.org/10.1016/j.biotechadv.2008.08.001.
31. **Gallagher MJ, Gallagher J, Vaze N, Gangoli S, Vasilets VN, Gutsol AF, Milovanova TN, Anandan S, Murasko DM, Fridman AA.** 2007. Rapid inactivation of airborne bacteria using atmospheric pressure dielectric barrier grating discharge. IEEE Trans Plasma Sci **35:**1501–1510. http://dx.doi.org/10.1109/TPS.2007.905209.
32. **Vaze ND, Gallagher MJ, Park S, Fridman G, Vasilets VN, Gutsol AF, Anandan S, Friedman G, Fridman AA.** 2010. Inactivation of bacteria in flight by direct exposure to non-thermal plasma. IEEE Trans Plasma Sci **38:**3234–3240. http://dx.doi.org/10.1109/TPS.2010.2072788.
33. **Park CW, Byeon JH, Yoon KY, Park JH, Hwang J.** 2011. Simultaneous removal of odors, airborne particles, and bioaerosols in a municipal composting facility by dielectric barrier discharge. Sep Purif Technol **77:**87–93. http://dx.doi.org/10.1016/j.seppur.2010.11.024.
34. **Liang Y, Wu Y, Sun K, Chen Q, Shen F, Zhang J, Yao M, Zhu T, Fang J.** 2012. Rapid inactivation of biological species in the air using atmospheric pressure nonthermal plasma. Environ Sci Technol **46:**3360–3368. http://dx.doi.org/10.1021/es203770q.
35. **Zimmermann JL, Dumler K, Shimizu T, Morfill GE, Wolf A, Boxhammer V, Schlegel J, Gansbacher B, Anton M.** 2011. Effects of cold atmospheric plasmas on adenoviruses in solution. J Phys D Appl Phys **44:**505201. http://dx.doi.org/10.1088/0022-3727/44/50/505201.
36. **Alshraiedeh NH, Alkawareek MY, Gorman SP, Graham WG, Gilmore BF.** 2013. Atmospheric pressure, nonthermal plasma inactivation of MS2 bacteriophage: effect of oxygen concentration on virucidal activity. J Appl Microbiol **115:**1420–1426. http://dx.doi.org/10.1111/jam.12331.
37. **Wu Y, Yao M.** 2013. In situ airborne virus inactivation by microwave irradiation. Chin Sci Bull **59:**1438–1445. http://dx.doi.org/10.1007/s11434-014-0171-3.
38. **Wu Y, Liang Y, Wei K, Li W, Yao M, Zhang J.** 2014. Rapid allergen inactivation using atmospheric pressure cold plasma. Environ Sci Technol **48:**2901–2909. http://dx.doi.org/10.1021/es5003988.
39. **Strauss JH, Sinsheimer RL.** 1963. Purification and properties of bacteriophage MS2 and of its ribonucleic acid. J Mol Biol **7:**43–54. http://dx.doi.org/10.1016/S0022-2836(63)80017-0.
40. **Kuzmanovic DA, Elashvili I, Wick C, O'Connell C, Krueger S.** 2003. Bacteriophage MS2: molecular weight and spatial distribution of the protein and RNA components by small-angle neutron scattering and virus counting. Structure **11:**1339–1348. http://dx.doi.org/10.1016/j.str.2003.09.021.
41. **Wang S, Wan J.** 2009. Oxygen effects on a He/O_2 plasma jet at atmospheric pressure. IEEE Trans Plasma Sci **37:**551–554. http://dx.doi.org/10.1109/TPS.2009.2012861.
42. **Yusupov M, Bogaerts A, Huygh S, Snoeckx R, van Duin AC, Neyts EC.** 2013. Plasma-induced destruction of bacterial cell wall components: a reactive molecular dynamics simulation. J Phys Chem C **117:**5993–5998. http://dx.doi.org/10.1021/jp3128516.
43. **Miura T, Yasuda H, Kurita H, Takashima K, Mizuno A.** 2012. Analysis of the inactivation mechanism of bacteriophage ϕX174 by atmospheric barrier discharge, p 1–4. Abstr Industry Appl Soc Annu Meet, IEEE. http://dx.doi.org/10.1109/IAS.2012.6373981.
44. **Peabody DS.** 1993. The RNA binding site of bacteriophage MS2 coat protein. EMBO J **12:**595.
45. **Laroussi M.** 2005. Low temperature plasma-based sterilization: overview and state-of-the-art. Plasma Processes Polym **2:**391–400. http://dx.doi.org/10.1002/ppap.200400078.